JOURNAL OF CATALYSIS 34, 257–266 (1974)

Charge Transfer During Redox of Bismuth Molybdate Catalysts*

K. M. SANCIER, A. AOSHIMA AND H. WISE

Stanford Research Institute, Menlo Park, California 94025

Received December 17, 1973

Charge transfer to and from silica-supported bismuth molybdate catalysts MoO_3, $Bi_2O_3 \cdot 3\ MoO_3 + 0.25\ Bi_2O_3$, $3\ Bi_2O_3 \cdot MoO_3$, and Bi_2O_3 (designated as M, B/M-0.7, B/M-6, and B, respectively) has been investigated by measuring the changes of the electrical conductance and of the ESR line due to Mo^{5+} during exposure of the catalysts to propylene or oxygen and during steady-state catalysis. For reduction by propylene at 600 and 660 K, the order of the initial charge transfer rates ($t < 5$ sec) of the catalysts are: B/M-0.7 > M > B/M-6 > B. Upon extended reduction ($t > 5$ sec) the order is unchanged at 660 K and at 600 K is reversed for catalysts B/M-0.7 and M. The initial rapid rate exhibited by catalyst B/M-0.7 is most likely due to reactive surface oxygen, while subsequent rates appear to be limited by bulk diffusion. Upon extended reduction of catalyst B/M-07 at 600 K, the electrical conductance increases continuously but according to ESR data the formation of Mo^{5+} ceases. At 660 K, the initial charge transfer rates upon reduction of catalysts M and B/M-0.7 are nearly the same. This behavior is ascribed to rapid exchange of bulk and surface oxygen.

The kinetics of charge transfer upon oxidation is analyzed in terms of a model in which the rate of incorporation of oxygen in the lattice depends on the oxygen vacancy concentration. Such an analysis demonstrates dissociative chemisorption of oxygen as a rate-limiting process. The temperature dependence of the charge transfer rates upon initial oxidation and reduction gives apparent activation energies of 18 kcal/mole for oxidation and 23 kcal/mole for reduction. The charge-transfer kinetics exhibit half-order dependence on oxygen and first-order dependence on propylene pressures.

During catalytic oxidation of propylene, the process of charge transfer is postulated to be associated with hydrogen removal from propylene by surface oxygen of the catalyst. Subsequent steps in the oxidation mechanism determine catalyst selectivity.

INTRODUCTION

The interpretations of the selectivity of bismuth molybdate catalysts for partial oxidation of olefins have been based on considerations that are primarily related to bulk characteristics of the catalysts, such as structure, composition, reducibility and oxidizability (*1–11*). In most of the reduction studies, the results show some disagreement as to the effect of catalyst composition on reducibility. Also, long-term exposure of the catalysts to reducing gases may cause bulk diffusion to become the rate-limiting reaction. In the oxidation studies, the oxidation rates have been too fast to permit adequate recording and interpretation of the event occurring at the surface.

The emphasis of the present study is on charge transfer reactions that may be expected to relate to the character of the surface during steady-state catalysis. We have examined the kinetics of charge transfer during initial oxidation and initial reduction of bismuth molybdate catalysts and during steady-state catalysis. The experimental approach employed the extended ESR technique (*12*), which is capable of simultane-

* This study was sponsored by a group of industrial companies whose support is gratefully acknowledged.

ously measuring the ESR Mo^{5+}-signal intensity and the rapid changes of electrical conductance of the catalysts. Since the measurements were made at microwave frequencies, the effect of electronic surface barriers on intergranular conductance was minimized.

Experimental Details

The detailed preparation of the catalysts has been previously described (*6*). The silica-supported catalysts have the following designations and compositions: M, MoO_3/77 wt% SiO_2; B/M-0.7, [$Bi_2O_3 \cdot 3MoO_3$ + 0.25 Bi_2O_3]/50 wt% SiO_2; B/M-6, $3Bi_2O_3 \cdot MoO_3$/50 wt% SiO_2; and B, Bi_2O_3/55 wt% SiO_2. In B/M-0.7 and B/M-6, the number following the letter designation signifies the approximate Bi/Mo atom ratio. Catalysts M and B/M-0.7 have equal weight fractions of molybdenum.

The catalytic reactor consisted of a quartz tube (3 mm o.d.) held vertically in one ESR cavity of a dual cavity. The bottom of the tube was constricted to provide a small opening (1 mm i.d.) which was plugged with quartz wool (3 mm long) to hold the column of powdered catalyst (about 0.1 g and 2.5 cm long) in place. The upper end of the reactor tube was secured into a Swagelock tee fitting which was adapted with a gas inlet and a rubber septum. Through the septum was inserted a ceramic tube (2 mm o.d.) containing a thermocouple in contact with the top of the catalyst column. Thus gas flowed downward through the catalyst bed and vented into the nitrogen stream of the temperature-controlled Dewar in the cavity. The temperature gradient across the catalyst was about 12 K at 575 K and 25 K at 675 K.

The reactant gases were provided in two streams, oxygen/helium and propylene/helium. The flow rates of the individual gases could be separately adjusted and the gas streams mixed. The gas-handling system also was equipped to provide abrupt changes in gas composition by means of a Loenco valve which could direct either stream to the reactor through a short length (30 cm) of copper tubing (0.15 cm i.d.). To minimize disturbances due to pressure differences upon switching streams, the back pressures of the stream not passing through the reactor was equalized to that passing through the reactor. The contact time of the gas with the catalyst at 600 K was estimated to be 0.1 sec for a flow of 50 cc/min.

During reaction conditions, measurements were made of (a) $\Delta I_{Mo^{5+}}$ the change in peak–peak intensity of the ESR line due to Mo^{5+} ions at a g value of about 1.93 (a weak Mo^{5+} signal was usually present even for oxidized samples), and (b) ΔV, which is proportional to the change in electrical conductance of the sample but which provides no information on the absolute conductance of the sample (*12*). Actually, ΔV is the change in the output voltage of the microwave crystal diode detector. An increase in

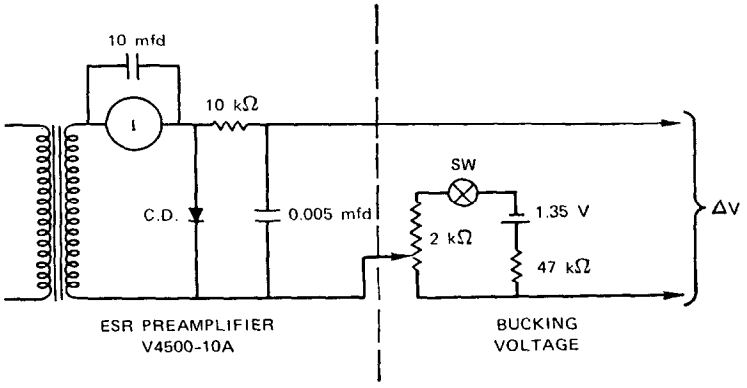

Fig. 1. Schematic wiring diagram for recording the crystal voltage. (1) Crystal current (leakage) meter; (C.D.) the microwave crystal diode.

ΔV corresponds to an increase in the electrical conductance of a sample as it is reduced by propylene, and a decrease of ΔV corresponds to a decrease in electrical conductance of the sample as it is oxidized by oxygen.

The schematic diagram of the circuit for recording ΔV is shown in Fig. 1. Two recorders were used: for relatively slow changes a Moseley Autograph 1700 BM (pen speed 0.5 sec full scale), and for rapid changes a Honeywell Visicorder 1508 equipped with a galvonometer with a 600-Hz response. An amplifier (Kintell 111BF with a gain of 10^3) was used to amplify the signal to the Visicorder.

The response time of the electronic circuits to conductance changes at the sample position was determined by inserting a silicon diode (IN4454, forward biased) in place of the sample. With no applied potential, the resistance of the diode was high ($10^6\ \Omega$). When a potential (1.5 V) was applied with a current limiting resistance ($150\ \Omega$) the resistance dropped to a low value ($10\ \Omega$) in about 10^{-9} sec. The increase in charge carriers in the diode caused an unbalance of the microwave bridge and a change in the crystal voltage (ΔV = 3 mV). In this way the time response of the entire electronic circuit was found to be about 2 msec, approximately that of the Visicorder. The response time of the Moseley recorder was 20 times faster than any event recorded by it.

The relative change in electrical conductance per oxygen molecule was evaluated by introducing a known aliquot of air through a rubber septum into the helium stream passing over a catalyst partially reduced by propylene at 660 K. The amount of oxygen removed from the aliquot was determined by gas chromatography (molecular sieve 5A, ¼ in. × 6 ft, room temperature) and by the change in ratio of oxygen-to-nitrogen peaks. For this determination the reactor was of an earlier design (*6*) that permitted chromatographic analysis of the exit gas. Assuming that oxygen reacts to form O^{2-}, we estimate that a 1 mV change of crystal voltage, ΔV, is equivalent to chemisorption of 6×10^{16} O_2 molecules or the transfer of 24×10^{16} electrons.

Results

The changes of the crystal voltage, ΔV, of four catalysts upon reduction by propylene at 600 K are shown in Fig. 2 and at 660 K in Fig. 3. Simultaneously, at 600 K the changes in the value of $\Delta I_{Mo^{6+}}$ were measured for each of the two catalysts (M and B/M-0.7) containing an equal amount of molybdenum (Fig. 4). At 660 K the reac-

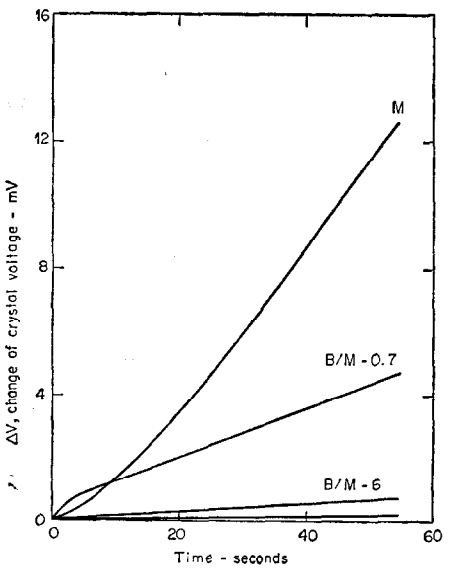

FIG. 2. Dependence of ΔV on propylene reduction of bismuth molybdate catalysts at 600 K. 44% C_3H_6 in He at 500 cc/min.

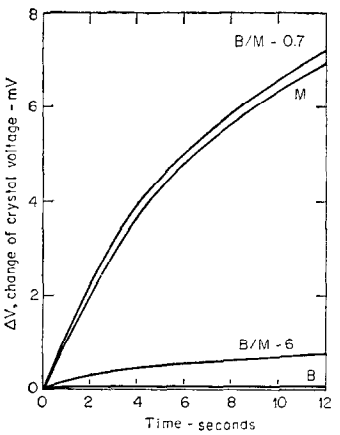

FIG. 3. Dependence of ΔV on propylene reduction of bismuth molybdate catalysts at 660 K. 44% C_3H_6 in He at 50 cc/min.

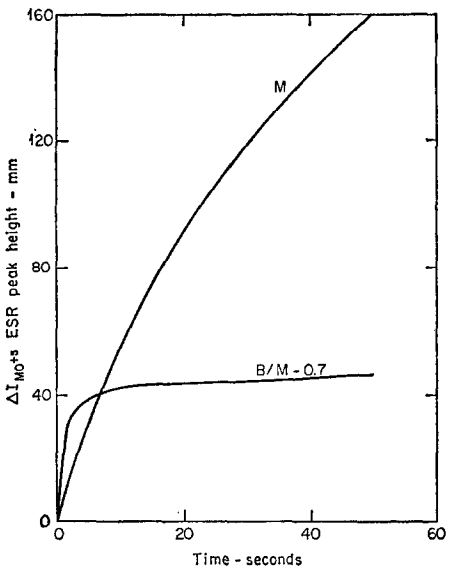

FIG. 4. Dependence of the change of I_{Mo}^{5+} on propylene reduction of bismuth molybdate catalysts at 600 K. 44% C_3H_6 in He at 50 cc/min.

tion rate was too fast to record $\Delta I_{Mo^{5+}}$. The catalysts were first equilibrated at 600 K for at least 10 min in a stream of O_2 (50 cc/min). When the crystal voltage attained a constant value, the oxygen was abruptly replaced by a propylene stream (44 vol% in He at 50 cc/min).

The changes of the crystal voltage upon the oxidation of the four catalysts at 600 K are shown in Fig. 5. The oxidation process was performed after the catalysts had been reduced to a given arbitrary value of ΔV (~7 mV) except for catalysts B and B/M-6, which could not be reduced as much in the given period of time (see Fig. 2). After the partial reduction, the propylene flow was stopped, and helium was flushed over the catalyst for about 1 min until the value of V remained essentially constant, then the gas stream was switched to pure oxygen. Repeated reductions and oxidations of a given catalyst gave reproducibility of ±5%.

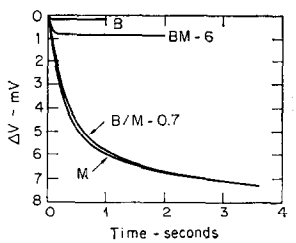

FIG. 5. Oxidation of catalysts at 600 K. 100% O_2 at 50 cc/min.

The rates of change of the crystal voltage $d\Delta V/dt$, for initial reduction and initial oxidation depend upon the propylene and oxygen concentration in the gas, as illustrated for catalyst M at 600 K in Fig. 6. The rate for oxidation is always much greater than for reduction at a given temperature and pressure of reactant gas.

The rates of change may be expressed by the kinetic equations:

$$\text{Reduction} \quad d\Delta V/dt = k_r P_{C_3H_6}, \qquad (1)$$

$$\text{Oxidation} \quad d\Delta V/dt = k_0 P_{O_2}^{1/2}, \qquad (2)$$

where k_r and k_0 are the rate constants corresponding to the reduction and oxidation processes, P is the pressure of the reactant and the exponent of P indicates the order of the reaction. The linear dependence $d\Delta V/dt$ on the square root of the oxygen concentration is examined further by a detailed analysis of the oxidation kinetics in terms of oxygen vacancy concentration (cf. Discussion).

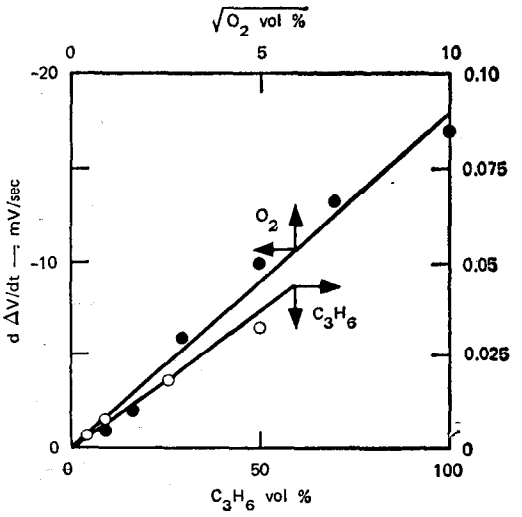

FIG. 6. Effect of gas composition on initial rates of conductance change (t = 0) for reduction (C_3H_6) and oxidation (O_2) of catalyst M at 600 K.

TABLE 1
RATE CONSTANTS FOR INITIAL REDUCTION AND OXIDATION OF CATALYSTS[a]

	k_r (mV sec^{-1} Torr^{-1} × 10^4)		k_0 (mV sec^{-1} Torr$^{-1/2}$)		k_r/k_0 (Torr$^{1/2}$ × 10^3)	
Catalyst	K: 600	660	600	660	600	660
M	2.2	30	0.62	0.73	0.35	4.2
B/M-0.7	8.4	34	0.51	0.69	1.7	5.0
B/M-6	0.42	2.3	0.26	0.21	0.16	1.1
B	0.11	0.24	0.19	—[b]	0.06	—

[a] Estimated probable error ±5%.
[b] Too small to estimate.

The values of k_r and k_0 were determined for the four catalysts at two reaction temperatures from the initial slopes of ΔV upon reduction and oxidation, and the results are tabulated in Table 1. At a given temperature, the value of the ratio k_r/k_0 exhibits a maximum for the catalyst B/M-0.7 and indicates that this catalyst is initially somewhat more reducible than the other catalysts. The rates of reduction determined from the ESR data of Fig. 4 also show that catalyst B/M-0.7 is initially more reducible than catalyst M, and by about the same ratio as determined from ΔV in Fig. 2.

The temperature dependences of the rate constants of the processes of oxidation and reduction of catalyst M are shown in Fig. 7. For the oxidation study, the catalyst at 600 K was reduced by propylene (4% in He) to a given value of ΔV, and then the catalyst was flushed with helium. After the catalyst temperature was decreased to the indicated value in the range from 375 to 600 K, an oxygen stream (5% in He) was introduced over the catalyst. In the reduction study the catalyst was first oxidized at 600 K and then reduced at the temperature indicated in the range from 560 to 600 K. The Arrhenius plots in Fig. 7 yield for the linear portions at high temperatures apparent activation energies of 18 kcal/mole for the oxidation process and 23 kcal/mole for the reduction process. It was ascertained that flushing with helium after reduction (or oxidation) had no subsequent effect on the kinetics of oxidation (or reduction). However, an atmosphere of helium caused slow reduction of the catalysts, as discussed below.

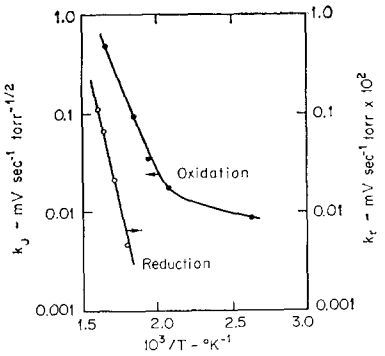

FIG. 7. Temperature dependence of rate constants for initial reduction and oxidation of catalyst M.

In the above analysis at various temperatures, it has been assumed that the measured changes in electrical conductance resulting from oxidation or reduction are independent of the actual electrical conductance which is temperature dependent.

It is of interest to determine the influence of catalyst composition on the extent of charge transfer and the extent of reduction of a catalyst during catalysis. One approach to this problem involves measurement of ΔV_s, the change of crystal voltage under steady-state catalytic conditions. In these experiments the total gas flow rate was maintained at 100 cc/min, the oxygen flow rate at 12 cc/min, and the flow rates of propylene and helium were adjusted to provide the desired ratio of O_2/C_3H_6. The results of such measurements are shown in Figs. 8 and 9 for the four catalysts at 660 K.

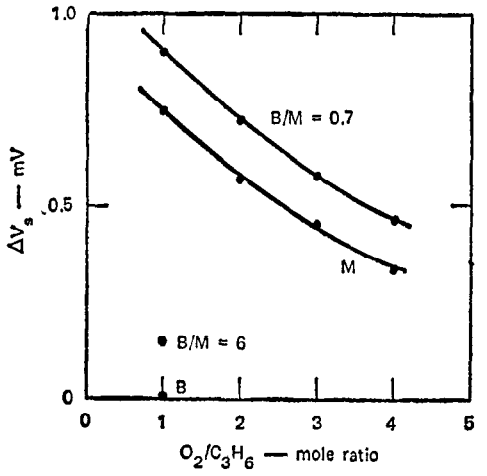

FIG. 8. Steady-state values of ΔV_s as a function of O_2/C_3H_6 mole ratio for four catalysts at 660 K. Total flow rate 100 cc/min O_2 at 12 cc/min, remainder C_3H_6 and He.

Before each measurement, the catalyst was exposed to oxygen until the crystal voltage was constant. The gas composition was then switched to a given ratio of O_2/C_3H_6 and the crystal voltage changed to a steady-state value of V_s. Under these steady-state conditions, it is evident that catalyst B/M-0.7 has the highest crystal voltage (i.e., highest electrical conductance). At 600 K, the values of ΔV were about 10% of those at 660 K, but the precision was not adequate to differentiate between catalysts M and B/M-0.7. For comparison, the ratios k_r/k_0 from Table 1 are also plotted in Fig. 9.

To obtain information on the ease of oxygen removal from these catalysts, helium was passed over the fully oxidized catalysts at 600 K and $I_{M^{5+}}$, the intensity of the ESR signal due to Mo^{5+}, was montiored. As shown in Fig. 10, $I_{Mo^{5+}}$ changed less and at a slower rate than that observed for the catalysts M and B/M-0.7 during reduction with propylene (Fig. 4). The value of the crystal voltage was not sufficiently stable over the long duration of the vacuum reduction experiment to obtain meaningful correlations of ΔV with catalyst composition.

The Mo^{5+} ESR resonance of a catalyst which has been partially reduced by propylene is subject to a magnetic dipolar broadening effect of gaseous oxygen. The signal intensity decreases rapidly (<1 sec) by about 25% when the oxygen pressure is suddenly increased; this effect is rapidly reversed as the oxygen pressure is decreased. This behavior is undoubtedly due to the fact that, for the partially reduced catalyst, some of the Mo^{5+} ions are at the surface where they can interact with the magnetic moment of oxygen molecules. However, such an effect is not observed for oxidized catalysts, such as were studied in the experiments of Figs. 4 and 10, for which the observable Mo^{5+} resonance is initially due to Mo^{5+} ions largely below the surface. Hence, the initial increases of $I_{Mo^{5+}}$ in these figures are due entirely to the reduction of the catalyst (by propylene or helium) and not to removal of broadening effects.

DISCUSSION

The observed changes in ΔV result from changes in the electrical conductance of the

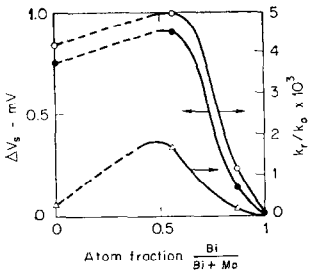

FIG. 9. Effect of catalyst composition on steady-state values of ΔV_s for $O_2/C_3H_6 = 1$ (●) and ratio of rate constants k_r/k_0 at 660 K (○); and of k_r/k_0 at 600 K (△).

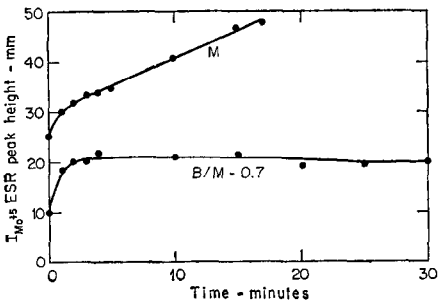

FIG. 10. Helium reduction of catalysts M and B/M-0.7 at 600 K. He flow 50 cc/min.

catalysts where an increase is associated with electron injection (reduction) to the catalyst and a decrease with electron removal (oxidation) from the catalysts. An increase of the Mo^{5+} resonance intensity indicates that Mo^{6+} ions have been reduced to Mo^{5+} ions or (the electrical equivalent) that oxygen ion vacancies are produced.

Initial and Steady-State Reduction

The absolute magnitude of the changes observed for these parameters indicates that the behavior of the catalysts differ markedly during reduction. For catalyst B/M-0.7 the initial rate of reduction by propylene at 600 K is larger than that of the other catalysts, and the trend is weaker but still discernible at 660 K (Fig. 3 and Table 1). This unusual behavior of catalyst B/M-0.7, especially at 600 K, suggests that there is a higher concentration of an electron accepting species on the catalyst surface, presumably an oxygen species, than on the surfaces of the other catalysts. Since at 660 K the reactivities are almost equal for catalysts B/M-0.7 and M, it appears that the surface concentration of the reactive oxygen is almost equal. This equivalence could occur if diffusion of oxygen from the bulk to surface was not rate limited at the higher temperature. However, bulk diffusion of oxygen cannot account for the greater reduction rate for catalyst B/M-0.7 than for catalyst M because the diffusion coefficient for molybdenum oxide is about double that for bismuth molybdate (*5*).

The slow initial rise of ΔV for catalyst M followed by a more rapid rise (Fig. 2) suggests an induction period for the reaction such as reported for a similar catalyst (*5*).

It appears that the initial charge transfer rates are not indicators of the activity or selectivity that differ significantly for catalysts B/M-0.7 and M at 660 K, a temperature approaching practical catalytic conditions. Accordingly, charge transfer must occur in an early step in the mechanism of propylene oxidation, and probably before (or with) the rate-limiting hydrogen-abstraction step in the formation of the allyl radical (*13*).

Long-Term Reduction

During prolonged propylene reduction of catalyst B/M-0.7, ($t > 5$ sec), the changes in ΔV (Fig. 2) and $\Delta I_{Mo^{5+}}$ (Fig. 4) seem to indicate two different processes. The regular increase of ΔV clearly results from progressive electron injection in the catalyst as higher density of donors are formed. On the other hand the Mo^{5+} resonance intensity attains a limiting value. Such behavior may be interpreted in terms of two models: (a) While the concentration of Mo^{5+} in the catalyst increases as reduction proceeds, only the surface Mo^{5+} ions are detectable by ESR at room temperature (*6*, *7*, *14*). According to this model, the ESR signal intensity is limited to the Mo^{5+} ions near the surface where the crystal field environment is of low symmetry. (b) The electrical conductance may arise, at least in part, from an impurity band in the semiconductor catalyst. Oxygen ion vacancies are likely to produce such an impurity band, which could be sufficiently below the bottom of the conduction band that ionization into the band would be limited at reaction temperatures. Morrison (*15*) postulates such an impurity band which "pins" the Fermi energy at an energy level comparable to the surface-state energy of the oxygen species involved in partial oxidation reactions. Such an impurity band could easily exist during steady-state catalysis, since we can estimate from the ΔV_s results that the degree of reduction of catalyst B/M-0.7 corresponds to a donor density of about 10^{18} cm^{-3}.† According to this model, reduction by propylene results in oxygen vacancies that form an impurity band and cause the electrical conductance to increase (e.g., as indicated by ΔV in Fig. 2). However, the concentration of Mo^{5+} will reach a constant value (Fig. 4) because ionization of the vacancy levels to the conduction band (to form Mo^{5+} species) is limited by the pinned Fermi energy.

† The extent of steady-state reduction leading to oxygen vacancies is estimated from $\Delta V_s = 0.5$ mV (catalyst B/M-0.7, and $O_2/C_3H_6 = 3$, cf. Fig. 8), the equivalence $\Delta V \equiv 1.2 \times 10^{17}$ oxygen vacancies/mV, and by taking into account that 0.1 g sample was used and its density is about 5 g/cm^3: $(0.5)(1.2 \times 10^{17})(5/0.1) = 3 \times 10^{18}$ cm^{-3}.

Kinetics of Initial Oxidation

The oxidation rate is greater than the reduction rate for a given reactant gas pressure by a factor of about 200 (Fig. 6). As shown in Table 1, the oxidation rates are almost equal for catalysts M and B/M-0.7 and the smaller values for catalysts B/M-6 and B probably arise from the small extent to which the catalysts were reduced.

We have examined the kinetics of the initial reoxidation of various catalysts (Fig. 5) by considering the interface reaction rate to be a function of the oxygen ion vacancies in the solid, a model similar to that used by Stotz (*16*). The composition of nonstoichiometric molybdenum oxide, MoO_{3-x}, may be expressed in terms of the oxygen-to-molybdenum ratio

$$n_O/n_M = 3 - x, \qquad (3)$$

where x represents the number of anion vacancies, n_O and n_M the number of g-atoms of the oxygen or molybdenum ions in the solid. If, for a specified gaseous oxygen pressure in contact with the solid, the nonstoichiometric equilibrium composition is given by

$$n_O/n_M = 3 - x'$$

then, for the conversion of MoO_{3-x} to $MoO_{3-x'}$ the rate of oxygen uptake is given by:

$$r = (1/A)(dn_O/dt), \qquad (4)$$

where A represents the surface area. After differentiation of Eq. (3) one may rewrite Eq. (4) as follows

$$-dx/dt = Ar/n_M. \qquad (5)$$

At small departures from the equilibrium composition, r may be considered to be proportional to $(x - x')$:

$$r = (x - x')(dr/dx)_p, \qquad (6)$$

where p represents the partial pressure of oxygen in the gas phase. Thus by substitution into Eq. (5), one obtains

$$-dx/dt = (A/n_M)(x - x')(dr/dx)_p, \qquad (7)$$

and on integration

$$\ln[(x - x')/(x_i - x')] = -\alpha t, \qquad (8)$$

where the subscript i refers to initial conditions, and α is defined as

$$\alpha \equiv (A/n_M)(dr/dx)_p.$$

Since the vacancy density is proportional to the conductivity of the solid, the change in vacancy density $x - x'$ is proportional to the change of electrical conductance $\Delta V' = V - V^I$, where V^I is the crystal voltage associated with the fully oxidized catalyst and V is the voltage associated with the catalyst at any time during the reaction with oxygen. Thus, the measurement of $\Delta V - \Delta V^I$ as a function of time allows evaluation of α for a given catalyst exposed to a specified oxygen environment. A typical plot of the experimental data is presented in Fig. 11. Values of α for different catalysts and various gaseous oxygen concentrations are summarized in Table 2.

The results show that the uptake of oxygen can be expressed in terms of a model in which oxygen ion vacancies are filled by oxygen derived from the gas phase. Again, catalysts M and B/M-0.7 show little difference in their respective response to oxygen uptake. Of special interest is the variation in relaxation time exhibited by catalyst M as a function of partial pressure of oxygen (Table 2). It will be noted that α varies linearly with the square root of the

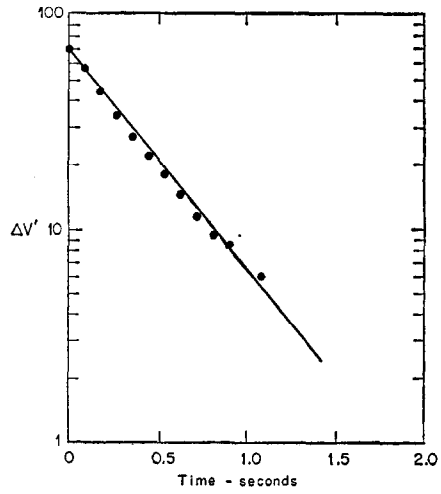

FIG. 11. Conductance change of catalyst B/M-0.7 during exposure to oxygen (temp = 600 K, oxygen pressure = 760 Torr).

TABLE 2
RELAXATION TIME FOR OXYGEN UPTAKE OF Bi/Mo OXIDE CATALYSTS AT 600 K

Catalyst	Oxygen pressure p (Torr)	Relaxation time α (sec^{-1})	$\alpha/p^{1/2}$
M	760	2.64	0.10
M	380	1.66	0.09
M	190	1.07	0.08
M	68	0.83	0.10
M	23	0.55	0.11
B/M-0.7	760	2.46	0.09
B/M-6	760	16.1	0.6

oxygen pressure, indicative of dissociative chemisorption as a rate-limiting step and subsequent formation of an oxygen radical anion species such as O^- or O^{2-}. Such a species is undoubtedly involved in the initial step of hydrogen abstraction from the propylene molecule. This result is in agreement with the square root dependence found from the measurements of the initial slopes of the oxidation reactions for different oxygen pressures (Fig. 6), and also reported by Adams (*17*).

Conceivably, the kinetics of initial oxidation could be described by a model in which oxygen dissociatively chemisorbs and produces a space charge that limits charge transfer. There are two reasons why this model is unsuitable: (a) chemisorption of oxygen over the range of $\Delta V = 7$ mV (Fig. 5) would lead to an unacceptably large surface concentration of about a monolayer of oxygen (e.g., as O_2^-), and (b) it is most unlikely that a simple mathematical model could account for chemisorption over the entire range of oxygen sorption (*18*).

In contrast to our findings that the rate of oxygen uptake of the catalysts depended upon oxygen pressure (α in Table 2), Matsuura and Schuit (*10*) reported that oxygen sorption on $Bi_2O_3 \cdot MoO_3$ in the temperature range of 300 to 670 K was independent of oxygen pressure. This difference is probably due to the difference in the character of the measurement: we measured charge transfer and Matsuura and Schuit measure amount of oxygen sorbed. Also, our catalysts were silica-supported whereas those of Matsuura and Schuit were not.

The kinetics of oxygen sorption based on the oxygen vacancy model is supported by the oxygen-18 tracer studies (*8*, *9*, *19*), which show that oxygen is rapidly transported between the bulk and the surface.

It is of interest to account for the rate-limiting steps which are associated with the activation energies of the initial charge transfer rates associated with oxidation and reduction (derived from Fig. 7). We have shown that oxygen chemisorption follows half-order kinetics; hence, the rate-limiting step associated with the 18 kcal/mole activation energy is probably due to dissociation of the oxygen molecule. By similar reasoning, the 23-kcal/mole activation energy is probably associated with the chemisorption of propylene, since such a process for conversion to acrolein is first-order in propylene. The rate-limiting step in this case may well be associated with allylic hydrogen abstraction (*17*) or with oxygen ion diffusion. Several workers have measured the activation energies for long-term oxidation (*10*, *14*) and reduction (*20*, *21*) processes on bismuth molybdate catalysts, but a wide range of values have been reported depending on catalyst preparation and catalyst composition.

CONCLUSIONS

From the measurement of charge transfer during initial reduction at 600 K, catalyst B/M-0.7 exhibits the highest rate of electron capture. At 660 K where the initial rates of charge transfer upon reduction for catalysts M and B/M-0.7 are almost equal, it is probable that charge transfer is no longer limited by bulk oxygen diffusion. We propose that charge transfer during reduction may involve hydrogen atom transfer from the propylene to the catalyst but precedes the steps that determine activity and selectivity.

During long-term reduction, the continuous increase of electrical conductivity is attributed to continuous formation of oxygen vacancies and Mo^{5+} ions. The fact that, for catalyst B/M-0.7, the ESR line due to Mo^{5+} reaches a limiting value (Fig. 4) may be accounted for in two ways: the oxygen vacancies form an impurity band which pins

the Fermi energy, limits the extent of ionization of the vacancies to the conduction band, and thus limits the concentration of Mo^{5+} ions; or, Mo^{5+} are produced throughout the bulk, but only those ions at the surface are observable by ESR. However, results from long-term exposure to propylene are probably less relevant to catalytic processes than the initial rate results which pertain to the surface reactions.

The kinetics of charge transfer during initial oxidation of partially reduced catalysts involve dissociative chemisorption of oxygen and formation of a monoatomic ion (O^- or O^{2-}). Bulk vacancy diffusion is not considered rate-limiting. The activation energy for charge transfer upon initial oxidation is associated with this dissociation step. The activation energy for charge transfer in initial reduction is attributed to chemisorption of propylene or to oxygen ion diffusion.

References

1. Sachtler, W. M. H., and DeBoer, N. H., *Proc. Int. Congr. Catal., 3rd* **1**, 254 (1965).
2. Otama, Hara, Funami, and Oda, *Shokubai* **11**, 125 (1969).
3. Pluta, J., *Z. Anorg. Allg. Chem.* **356**, 105 (1967).
4. Peacock, J. M., Parker, A. J., Ashmore, P. G., and Hockey, J. A., *J. Catal.* **15**, 387 (1969).
5. Batist, Ph. A., Kapteijns, C. J., Lippens, B. C., Schuit, G. C. A., *J. Catal.* **7**, 33 (1967).
6. Sancier, K., Dozono, T., and Wise, H., *J. Catal.* **23**, 270 (1971).
7. Burlamacchi, L., Martin, G., and Ferroni, E., *J. Chem. Soc. Faraday Trans. I*, **68**, 1586 (1972).
8. Keulks, G. W., *J. Catal.* **19**, 232 (1970).
9. Wragg, R. D., Ashmore, P. G., and Hockey, J. A., *J. Catal.* **22**, 49 (1971).
10. Matsuura, I., and Schuit, G. C. A., *J. Catal.* **20**, 19 (1971).
11. Batist, Ph. A., Van de Moesoijk, C. G. M., Matsuura, I., and Schuit, G. C. A., *J. Catal.* **20**, 45 (1971).
12. Setaka, M., Sancier, K. M., and Kwan, T., *J. Catal.* **16**, 44 (1970).
13. Adams, C. R., and Jennings, T. J., *J. Catal.* **3**, 549 (1964).
14. Egashira, M., Sumie, H., Sakamoto, T., and Seiyama, T., *Kogyo Kagaku Zasshi* **73**, 860 (1970).
15. Morrison, S. R., unpublished data.
16. Stotz, S., *Ber. Bunsenges.* **70**, 769 (1966).
17. Adams, C. R., *Proc. Int. Congr. Catal., 3rd* **1**, 240 (1965).
18. Weisz, P. B., *J. Chem. Phys.* **21**, 1571 (1953).
19. Novakova, J., and Jiru, P., *J. Catal.* **27**, 155 (1972).
20. Peacock, J. M., Parker, A. J., Ashmore, P. G., and Hockey, J. A., *J. Catal.* **15**, 398 (1969).
21. Keulks, G. W., Rosynek, M. P., and Daniel, C., *Ind. Eng. Chem. Prod. Res. Develop.* **10**, 138 (1971).